APPLIED ORGANOMETALLIC CHEMISTRY
Appl. Organometal. Chem. 2007; **21**: 246–254
Published online in Wiley InterScience
(www.interscience.wiley.com) DOI:10.1002/aoc.1188

Molecular photochromic systems: a theoretical and experimental investigation on zinc(II) dithizonate

L. Armelao[1]*, G. Bandoli[2], D. Barreca[1], G. Bottaro[1], E. Tondello[3], A. Venzo[1] and A. Vittadini[1]

[1]ISTM-CNR and INSTM, Dipartimento di Scienze Chimiche, Università di Padova, 35131 Padova, Italy
[2]Dipartimento di Scienze Farmaceutiche, Università di Padova, 35131 Padova, Italy
[3]Dipartimento di Scienze Chimiche, Università di Padova and INSTM, 35131 Padova, Italy

Received 20 November 2006; Accepted 20 November 2006

Zinc(II)-dithizone based molecular systems [$Zn(HDz)_2$] are intriguing candidates for the development of optical devices thanks to their interesting photochromic and nonlinear optical properties. In the present work, the behavior of $Zn(HDz)_2$ in different solvents was investigated by a combined theoretical and experimental approach. In particular, solutions of both dithizone (H_2Dz) and $Zn(HDz)_2$ were analyzed by optical absorption spectroscopy and nuclear magnetic resonance (NMR) techniques, with particular attention to structure–properties relationships. Density functional and time-dependent density functional calculations were performed on the stable and the activated forms of the complex, obtaining information on the energetics of their interconversion, as well as on the nature of their electronic excitations. Copyright © 2007 John Wiley & Sons, Ltd.

KEYWORDS: Zinc(II) dithizonate; optical properties; NMR; density functional theory

INTRODUCTION

Diphenylthiocarbazone, or dithizone [1,5-diphenyl-3-formazathiol, H_2Dz], is a diprotic organic acid which forms strongly colored complexes with most transition metals.[1] In particular, different coordination compounds of the monoanionic HDz^- species in tetrahedral or square-planar geometries [$M(HDz)_2$, M = Zn, Cd, Hg, Pt, etc.] have been previously synthesized and characterized.[2] The interest towards such compounds has been notably stimulated by their photochromism, i.e. the reversible interconversion between two molecular forms endowed with different absorption properties, observed both under UV–vis steady illumination[3,4] and laser pulse photolysis.[5] The color change from red to violet blue is usually regarded as an inherent property of the HDz^- ligand, since the involved electronic transitions are essentially localized on its molecular orbital system, whereas the nature of metal centers seems to influence only the speed of the interconversion process.[6] The photochromic interconversion opens appealing possibilities for the use of the above complexes in various fields. In fact, solid-state systems containing photochromic molecules have displayed photoinduced birifrangence and dichroism phenomena[7] and can be proposed for the conception of data storage and opto-optical switching devices.[8–10] Besides, $M(HDz)_2$ molecular systems display remarkably large first and second molecular hyperpolarizabilities, which, in connection with the high absorption coefficients of the two forms involved in the photochromic process, play a prominent role for potential applications in nonlinear optics (NLO). In particular, the coupling between photochromism and NLO properties leads to specific material features that might be advantageous for several technological applications, such as reversible information storage, holography and all-optical modulators.[8–10] Further interesting perspectives for advanced applications might be offered by the exploitation of NLO properties for both the forms involved in the photochromic interconversion.

In this context, the tetrahedral Zn(II) dithizonate complex has been the subject of thorough investigations regarding its structure and chemical properties.[3,4,11,12] Fundamental studies on this system are simplified by the d^{10} closed shell of

*Correspondence to: L. Armelao, ISTM-CNR and INSTM, Dipartimento di Scienze Chimiche, Università di Padova, 35131 Padova, Italy.
E-mail: armelao@chin.unipd.it
Contract/grant sponsor: National Research Council.
Contract/grant sponsor: University of Padova.
Contract/grant sponsor: INSTM.

Zn(II), which avoids complications arising from metal–ligand electronic exchanges in the photochromic switching. The above compound presents photochromic activity not only in solution, but even in the solid state or when embedded as *guest* in polymer matrices.[13] Moreover, $Zn(HDz)_2$ films prepared by vacuum sublimation have been considered as potential candidates for erasable optical memories and optical modulators.[14] The structural analysis of the two forms involved in the photochromic transition for this system date back to the 1960s,[3,4] and the geometry of the excited species has been deduced by IR measurements on the irradiated form. Nevertheless, despite the initial attention, no conclusive studies on the photochromic process involving $Zn(HDz)_2$ have ever been reported.

In this framework, the present work is part of a research project aimed at the development of optical devices based on $Zn(HDz)_2$ embedded in transparent matrices. In particular, our attention is here focused on both the solution behavior of the $Zn(HDz)_2$ complex and the H_2Dz ligand, with the aim of further elucidating their optical properties for successive applications in solid-state systems. This study has been undertaken by combining theoretical and experimental investigation. In particular, the synthesis of Zn(II)–dithizone complex and its structural and chemical characterization have been performed. Subsequently, the behavior of $Zn(HDz)_2$ in various organic solvents, namely tetrahydrofurane, chloroform and ethyl acetate, was investigated by one- and two-dimensional ^1H and ^{13}C NMR spectroscopy and UV–vis optical absorption spectroscopy. Furthermore, *ab-initio* calculations were performed both on the Zn(II) complex and the uncoordinated ligand in the framework of time-dependent density functional theory (TDDFT).

EXPERIMENTAL

Chemicals

Zinc(II) acetate dihydrate (Alfa Aesar, 98 + %), ammonia (Alfa Aesar 28% w/w aqueous solution), ammonium chloride (Alfa Aesar, 98 + %) and dithizone (Sigma-Aldrich, ≥98%) were used as supplied without further purification.

Synthesis

Zinc(II) dithizonate was prepared according to a previously reported procedure.[15] A 0.51 g aliquot of $Zn(CH_3COO)_2 \cdot 2H_2O$ was dissolved in an ammonia solution obtained by mixing 6 ml of NH_3 25% (13.1 M) and 4.20 g of NH_4Cl, and adding distilled water up to a total volume of 20 ml. A second solution [1.7 g of dithizone (H_2Dz) in 40 ml of CH_3CH_2OH] was then slowly added under vigorous stirring, resulting in the instantaneous formation of a dark-red precipitate. After 10 min, the solid was filtered off and dissolved in 40 ml of $CHCl_3$. After liquid concentration, 50 ml of absolute ethanol were added and heating was continued up to the formation of the first bluish-green crystals from the solution. After 24 h at room temperature, the green-gray precipitate was isolated by filtration, washed in ethanol and dried under vacuum. The compound was finally purified by crystallization from $CHCl_3$ (overall yield = 60%).

Elemental analysis

Calculated for $C_{26}H_{22}N_8S_2Zn$: C, 54.2%; H, 3.9%; N, 19.4%; S, 11.1%. Found: C, 53.8%; H, 3.8%; N, 19.1%; S, 12.6%.

Characterization

Optical absorption spectra were recorded at room temperature on $Zn(HDz)_2$ solutions in tetrahydrofurane, chloroform and ethyl acetate in the 300–800 nm range on a double-beam CARY 5E UV–vis spectrophotometer with a spectral bandwidth of 1 nm. The solvent contribution was subtracted.

XRD measurements were made on a Nicolet Siemens R3m/V four-circle diffractometer with graphite-monochromated Mo-Kα radiation, under ambient conditions. The crystal batch had inherent difficulties and the only suitable sample for a single-crystal structure determination was sub-standard, as shown by the low number of observed data (only one-third of the total), due to the poor diffraction by the crystal at high angles. The structure was solved by direct method and expanded using Fourier techniques. The non-hydrogen atoms were refined anisotropically using full-matrix least-squares method on all F^2. The two H atoms involved in interaction with sulfur atoms were located in electron density map and refined. The remaining H atoms were placed in idealized positions and allowed to ride with the C atoms to which each was bonded. A summary of the crystallographic data is given in Table 1, while relevant bond distances and angles are reported in Tables 2 and 3.

^1H- and ^{13}C-NMR spectra were recorded using as solvents $CDCl_3$ at 298 K and 1 : 1 mixtures of $CDCl_3$ and CD_2Cl_2 at lower temperatures. The spectra were obtained using a Bruker Avance-400 spectrometer (operating at 400.13 MHz on ^1H and at 100.61 MHz on ^{13}C) equipped with a 5 mm inverse probe and a BVT-100 temperature controller. The chemical shift values are given as δ against internal tetramethylsilane (TMS) as reference. The assignments of the proton resonances were performed by standard chemical shift correlations and NOESY (nuclear Overhauser enhancement spectroscopy) experiments. The ^{13}C resonances were attributed by means of two-dimensional heterocorrelated experiments: HMQC (heteronuclear multiple quantum correlation) with bilinear rotation-decoupling (BIRD) sequence[16] and quadrature along F1 achieved using the time-proportional receiver phase incrementation (TPPI) method[17,18] and HMBC (heteronuclear multiple bond correlation)[19] methods for the H-bonded carbon atoms and the quaternary C ones, respectively. Relaxation delays of at least 10 s between the 90° pulses have been used to ensure correct signal integration in ^1H spectra. 2D-EXSY (exchange spectroscopy) experiments with a mixing time (τ_m) between 300 and 600 ms were acquired at different temperatures in the range 277–333 K, using the phase-sensitive NOESY[20] pulse sequence. Typically a data

DOI: 10.1002/aoc

Table 1. Crystallographic data and experimental parameters for the structure of $Zn(HDz)_2$

Molecular formula	$C_{26}H_{22}N_8S_2Zn$
Molecular weight	576.01
Crystal system	Monoclinic
Space group	$P\,2_1/c$
a, Å	7.875(2)
b, Å	22.352(5)
c, Å	15.217(3)
β, deg	92.60(3)
v, Å^3	2678.8(9)
z	4
D_{calcd}, g/cm^3	1.430
μ (Mo Kα), cm^{-1}	11.05
λ (Mo Kα), Å	0.71073
Θ (deg) range	3.5–25.1
Independent reflections	4721
Observed reflections [$I > 2\sigma(I)$]	1488
R[a] (obs. reflections)	0.032
R_w[b] (obs. reflections)	0.040
Highest residual, e Å^{-3}	0.16

[a] $R = \Sigma||F_o| - |F_c||/\Sigma|F_0|$; [b] $R_w = \{\Sigma[w(F_0^2 - F_c^2)]/\Sigma[w(F_0^2)^2]\}^{1/2}$.

Table 2. Selected bond distances for the $Zn(HDz)_2$ structure

Bond	Distance, Å	Bond	Distance, Å
Zn–S(1)	2.267(2)	Zn–S(2)	2.264(2)
Zn–N(1)	2.060(5)	Zn–N(5)	2.064(5)
N(1)–N(2)	1.281(6)	N(5)–N(6)	1.276(6)
N(1)–C(2)	1.427(7)	N(5)–C(15)	1.415(7)
N(2)–C(1)	1.372(7)	N(6)–C(14)	1.380(7)
C(1)–N(3)	1.312(7)	C(14)–N(7)	1.335(7)
N(3)–C(4)	1.322(6)	N(7)–N(8)	1.315(6)

matrix of 256 FIDs by 1K complex points was collected. Before transformation, the data points were multiplied by a square sine window function and zero filled to 2K × 2K real points. All the data treatments were performed on a Silicon Graphics *Indy* workstation using the X-WINNMR® rel. 2.5 software of Bruker Corp. For atom labeling, see Scheme 1.

Zinc(II) dithizonate

^{1}H-NMR ($\nu_0 = 400.13$ MHz; solvent, $CDCl_3$; T, 298 K; ppm from internal Me_4Si): δ 9.92 (s, 2H, NH), 7.51 (m, 4H, H_1), 7.42 (m, 4H, H_2), 7.19 (m, 2H, H_3), 7.79 (m, 4H, H'_1), 7.29 (m, 4H, H'_2), 7.33 (m, 2H, H'_3).

^{13}C-NMR ($\nu_0 = 100.61$ MHz; solvent, $CDCl_3$; T, 298 K; ppm from internal Me_4Si): δ 119.98 (C_1), 130.54 (C_2), 125.75 (C_3), 123.43 (C'_1), 131.41 (C'_2), 103.57 (C'_3), 142.25 (C_A), 149.95 (C_B), 190.82 (C_0).

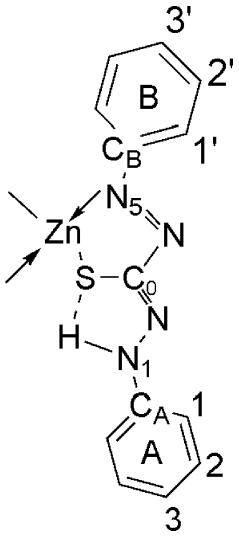

Scheme 1. Atom labeling for dithizone employed in the present work.

Dithizone

^{1}H–NMR ($\nu_0 = 400.13$ MHz; solvent, $CDCl_3$; T, 298 K; ppm from internal Me_4Si): δ 12.53 (s, 2H, NH), 7.72 (m, 4H, H_1), 7.51 (m, 4H, H_2), 7.37 (m, 2H, H_3). ^{13}C–NMR ($\nu_0 = 100.61$ MHz; solvent, $CDCl_3$; T, 298 K; ppm from internal Me_4Si): δ 119.86 (C_1), 130.88 (C_2), 129.61 (C_3), 140.52 (C_A), 172.35 (C_0).

Theoretical calculations were performed with ADF 2002,[21–23] a suite of programs based on the density functional theory (DFT). Ground state energies and structures as well as interconversion paths were determined by using the so-called BLYP functional. Excitation energies were computed through TDDFT.[24,25] Triple-$\dot{\zeta}$ Slater-type orbital basis sets were used for all the atoms. These include the following polarization functions: a 2*p* orbital for H, a 3*d* orbital for C and N, and S. The 1*s* orbitals of C and N, the 1*s*–2*p* orbitals of S and Zn were orthogonalized against the valence ones and kept frozen throughout the calculations. Solvent effects were introduced by the COSMO continuum model as implemented in ADF.[26,27]

RESULTS AND DISCUSSION

Dithizone

Although dithizone (H_2Dz) was discovered about 100 years ago,[28] the electronic properties and the underlying geometric structure have been the subject of debate for several years. H_2Dz was represented in terms of a tautomeric equilibrium between the *enol* and *keto* forms until structural studies[29–31] unequivocally established its almost planar structure belonging to the C_{2v} point group, with the C–S bond lying on the intersection of the mirror planes (Fig. 1). Information obtained from the present one- and two-dimensional ^{1}H and ^{13}C-NMR measurements on H_2Dz

DOI: 10.1002/aoc

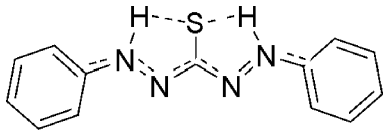

Figure 1. Schematic representation of the dithizone (H_2Dz) molecular structure.

solutions support this structure, due to the equivalence of the two imino protons, as well as of the two phenyl rings. The chemical shift of the former denotes the presence of a strong interaction via hydrogen bonding with the sulfur atom,[31] since their signal disappears completely upon treatment with D_2O or MeOD.

The visible electronic spectrum of H_2Dz[32–36] is characterized by two intense absorptions at $\lambda = 440–450$ nm and 605–625 nm, whose position strongly depends on the solvent nature and concentration. Attempts to reproduce the observed spectral bands were carried out by quantum chemical calculation,[6] but satisfactory results were obtained only recently, when the band located at 620 nm was reproduced for the first time.[37] The present calculations are in substantial agreement with those reported in Schönherr *et al*.[37] predicting the symmetric form of H_2Dz to be the most stable. An interesting point concerns the solvent effect on the position of the first absorption peak. According to Schönherr *et al*.,[37] a correct position for the peak could be obtained by explicitly introducing six solvent (methanol) molecules, concluding that specific hydrogen bonding effects were responsible for the discrepancy between the computed gas-phase excitation energies and those experimentally obtained in solution. Nevertheless, such a conclusion seems to be rather questionable, because similar discrepancies are observed even on using solvents unable to play any role in hydrogen bonding (e.g. CCl_4). In fact, theoretical results approach more closely the experimental ones by introducing a continuum model for the solvent. Such calculations have been performed for several solvents, yielding an improved agreement with the experiment, with a red-shift from a minimum of 124 nm (for CCl_4) to a maximum of 236 nm (for CH_3OH and CH_3CN).

Zinc dithizonate

X-ray analysis (Fig. 2) revealed that the $Zn(HDz)_2$ molecule contains two ligand groups coordinated to zinc trough sulfur and nitrogen, forming two five-membered chelate rings around the metal atom. These rings are almost planar (torsion angles between −4.9° and 6.7°) and orthogonally displaced (dihedral angle of 96°). The bond lengths, angles and atom labeling are given in Tables 2 and 3.

Both ligands display the same stereochemistry. The torsion angles in $C_{Ph}–N{=}N–C{=}N–N–C_{Ph}$ are within −178.2° and 177.3°, whereas the sum of angles around C(1) and C(14) is 359.9° in both ligands (Fig. 2). All the light atom–light atom bonds contain some degree of double bond character, which maintains the phenyl ring (B) coplanar with the five-membered chelate ring (dihedral angle of 9.7°), to which it is attached through N(3) and N(4). Likewise, phenyl group A maintains the coplanarity, being attached through N(1) to the

Table 3. Selected bond angles for the $Zn(HDz)_2$ structure

Bonds	Angle, deg	Bonds	Angle, deg
S(1)–Zn–N(1)	86.9(2)	S(2)–Zn–N(5)	86.5(2)
Zn–S(1)–C(1)	92.4(2)	Zn–S(2)–C(14)	92.8(2)
Zn–N(1)–C(2)	127.1(4)	Zn–N(5)–C(15)	128.1(4)
Zn–N(1)–N(2)	117.7(4)	Zn–N(5)–N(6)	118.4(4)
N(2)–N(1)–C(2)	115.1(5)	N(6)–N(5)–C(15)	113.5(5)
S(1)–C(1)–N(2)	125.9(5)	S(2)–C(14)–N(6)	126.2(5)
N(1)–N(2)–C(1)	119.6(5)	N(5)–N(6)–C(14)	115.8(5)
C(1)–N(3)–N(4)	117.3(6)	C(14)–N(7)–N(8)	117.4(6)
N(3)–N(4)–C(8)	120.9(6)	N(7)–N(8)–C(21)	120.1(6)
N(2)–C(1)–N(3)	109.3(6)	N(6)–C(14)–N(7)	109.1(6)
S(1)–C(1)–N(3)	124.7(5)	S(2)–C(14)–N(7)	124.6(5)

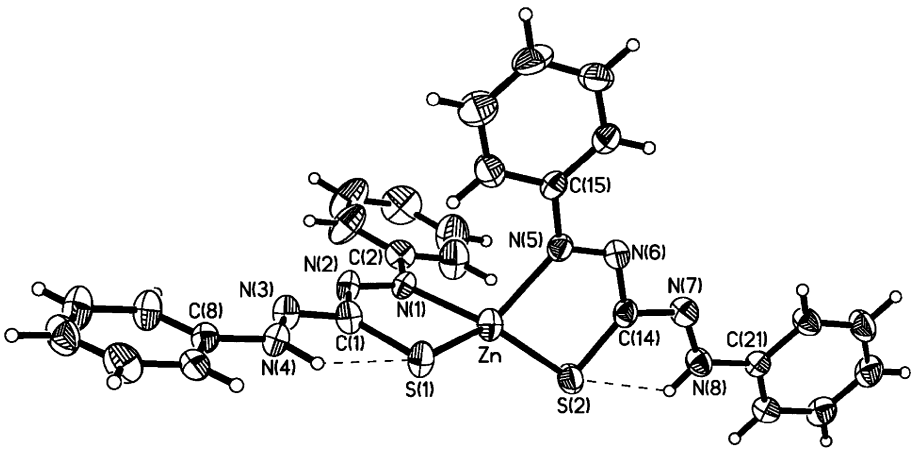

Figure 2. Structure of the $Zn(HDz)_2$ molecule. The S(1)···H(4) (at 2.44´Å) and S(2)···H(8) (at 2.51´Å) interactions are shown.

DOI: 10.1002/aoc

chelate rings (dihedral angle of 8.9°). As a consequence, the molecule can be visualized as resulting from two planes through A-zinc-B and A′-zinc-B′, tetrahedrally displaced around the metal atom and intersecting at 84.7°, deviating by only a few degrees from ideality.

One- and two-dimensional ^{1}H- and ^{13}C-NMR studies on $Zn(HDz)_2$ have been carried out in order to obtain a thorough characterization of its behavior in solution. The ^{1}H and ^{13}C chemical shift values are reported in the Experimental section. In the temperature range 195–333 K, NMR spectra display well-resolved signals due to two non-equivalent phenyl rings, and only one signal due to the imino protons at δ 9.92. The ^{1}H resonances were assigned by correlation spectroscopy measurements, and the relative position of the two rings was obtained by phase sensitive ^{1}H–^{1}H NOESY experiments. Both the X-ray data and the ^{1}H chemical shift value of N–H proton indicate that it is strongly hydrogen bonded to the sulfur atom, an interaction very similar to that occurring in H_2Dz (see above). The observed upfield shift by ca. 2.6 ppm with respect to H_2Dz can be attributed to the presence of the Zn–S bond, which decreases the negative charge density on the sulfur atom, thus lowering the strength of H···S hydrogen bond.

One-dimensional ^{1}H-NMR measurements have been performed up to 333 K with the aim of observing coalescence and re-sharpening of the signals; nevertheless, any eventual exchange process is slow even at 333 K and higher temperatures should be necessary. Line shapes and chemical shift values do not undergo significant variations in the δ range between 0 and 13 ppm, as depicted in Fig. 3. As a consequence, the most common line shape analysis,[38–42] applicable to processes with rate constants between 10^{1} and 10^{4} s^{-1}, is not useful in the present case. In order to study exchanging systems with rate constants between 10^{-2} and 10^{2} s^{-1}, 2D-EXSY measurements[43] present significant advantages. At variance with the line-shape analysis, chemical shift or line width measurements in the slow exchange limit, which is often inaccessible, are not necessary.

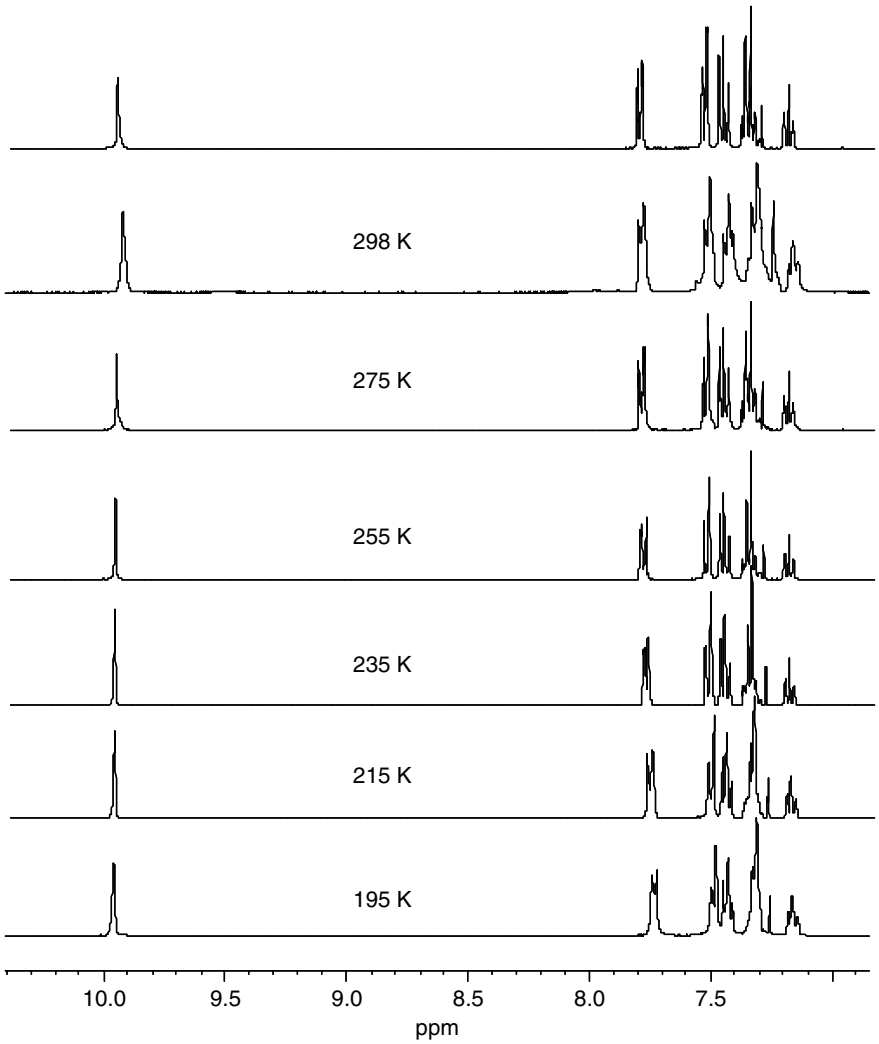

Figure 3. Low field region of ^{1}H-NMR spectra of $Zn(HDz)_2$ in $CDCl_3$ at selected temperatures (ν_o = 400 MHz).

DOI: 10.1002/aoc

Moreover, site-to-site rate constants can be evaluated from integration of the exchange cross-peaks,[44–46] yielding information on the mechanisms of exchange processes.

In the present work, 2D-EXSY experiments have been performed in the temperature range 255–333 K (Fig. 4). Below 273 K, the kinetics is too slow to yield useful EXSY cross peaks, as shown in Fig. 4(b) for $T = 255$ K. Conversely, at higher temperatures resolution of the off-diagonal peaks allows integration with an accuracy within ±10%. Mathematical treatment of the data affords the kinetic constants, k, reported in Table 4, together with the $\Delta G^{\neq}$, $\Delta H^{\neq}$, $\Delta S^{\neq}$ and the activation energy of the reaction obtained from an Eyring plot.

The observed behavior is consistent with a stereochemical inversion at the metal center, an exchange process already known in literature. Thirty years ago, Eaton and Holm[47] pioneered an investigation on the stereochemical non-rigidity of a series of bis(β-aminothionato)zinc(II) and cadmium(II) tetrahedral complexes. These metal chelates derived from unsymmetrical ligands are enantiomeric with absolute configurations Δ and Λ and undergo inversion at the metal center with subsequent racemization (Fig. 5).

Table 4. Rate constant and activation parameters of the exchange process in $Zn(HDz)_2$ solutions

T, K	Rate constant, s^{-1}[a]	$K^{\neq}$[b]	τ_m, s
333	2.20 ± 0.21	3.18×10^{-13}	0.3
318	1.18 ± 0.19	1.78×10^{-13}	0.3
298	0.52 ± 0.07	8.44×10^{-14}	0.6
287	0.39 ± 0.08	6.55×10^{-14}	0.5
277	0.27 ± 0.07	4.75×10^{-14}	0.5

$\ln A = 11.0 \pm 0.8\ s^{-1}$; $E_a = 6.8 \pm 0.4$ kcal × mol^{-1}. $\Delta G^{\neq}$ (298 K) = 17.8 ± 1.4 kcal mol^{-1}. $\Delta H^{\neq} = 6.2 \pm 0.4$ kcal mol^{-1}. $\Delta S^{\neq} = -46.0 \pm 1.5$ cal mol^{-1} K^{-1}.
[a] Determined by 2D-EXSY experiments in $CDCl_3$ solutions.
[b] Determined using the Eyring equation.

The processes proposed to explain such a behavior include: (i) intramolecular twist rearrangement generating a square planar transition state and proceeding without metal–ligand bond cleavage; (ii) intramolecular M–L bond cleavage-formation process through a tri-coordinated transition state; and (iii) intermolecular ligand exchange reaction. As a matter

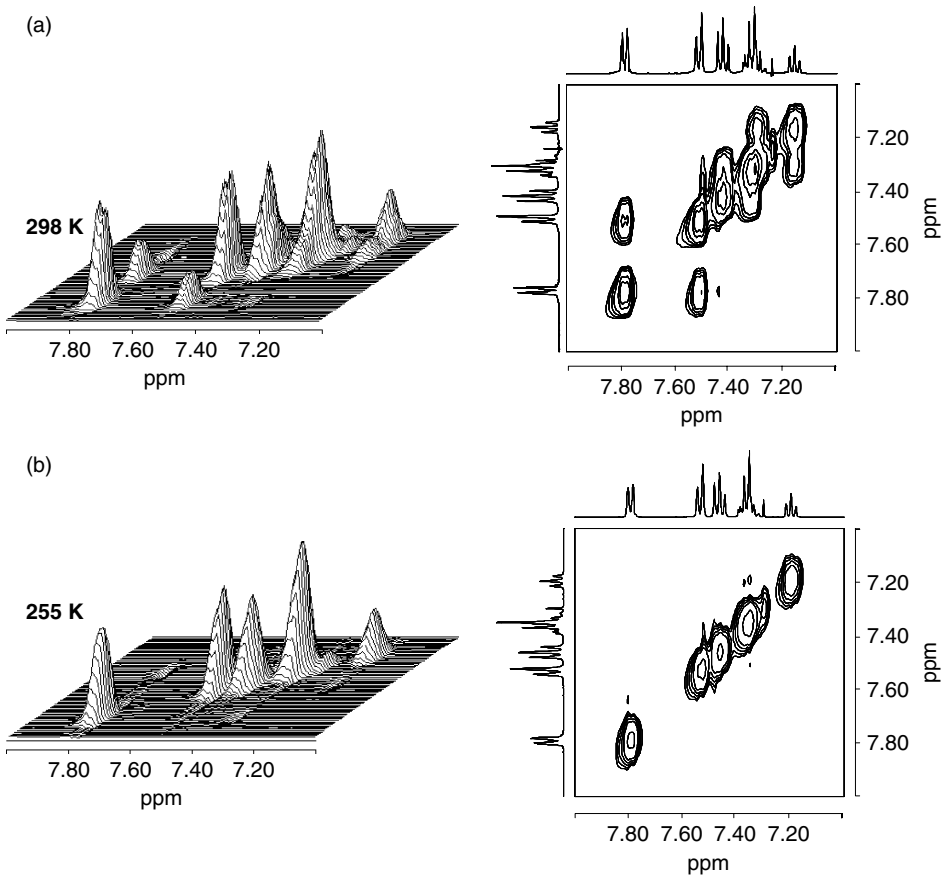

Figure 4. Two-dimensional stacked and normal plots of 2D-EXSY experiments recorded at 298 K (a) and 255 K (b) on $Zn(HDz)_2$ solution in $CDCl_3$. In both figures, the low field region is displayed only with positive levels in order to avoid confusion between NOE and exchange cross peaks.

DOI: 10.1002/aoc

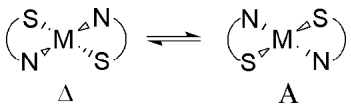

Figure 5. Schematic representation of the intramolecular enantiomerization process in $M(HDz)_2$ complexes.

of fact, the predominant mechanism and the corresponding rates are mainly influenced by the nature of the metal center. As concerns Zn complexes, a polytopal twist motion mechanism via *trans*-square planar intermediate has been suggested.[47,48]

The kinetic data on $Zn(HDz)_2$ dynamics agree with previous findings.[43–45] The energy barrier of the intramolecular enantiomerization process (E_a, see Table 4) indicates that intramolecular twist rearrangement with a square planar transition state is the most conceivable mechanism for the enantiomerization process.

Zinc(II) dithizonate displays an optical absorption spectra characterized by a single strong band centered at $\lambda = 532$ nm.[3,4] Under illumination, a second band at $\lambda \approx 610$ nm attributed to the activated form is observed and subsequently disappears when the pumping laser is turned off. The analysis of time-dependent spectral changes in the return reaction of the metal dithizonates has revealed a single isosbestic point showing the absence of reaction intermediates.[3,4] Therefore, the photochromic equilibrium is likely to involve only two forms, i.e. the stable and the activated one. This feature is typical for the $M(HDz)_2$ compound (M = Zn, Hg, Bi, Pt, Pd, etc.) and it is attributed to a structural isomerization of the ligand (Fig. 6). Based on spectral and kinetic studies, Meriwether *et al*.[3] proposed for the first time the structure of the activated form. The photochromic transformation should involve a *trans–cis* isomerization about the C–N bond and an N-to-N hydrogen transfer.

In order to compare the structure and stability of the activated form proposed by Meriwether *et al*.[4] with those of the stable one, computational experiments have been carried out in the framework of the DFT theory. Both isomers were fully optimized in the C_2 point symmetry group. The theoretical structure of the stable form agrees to a good

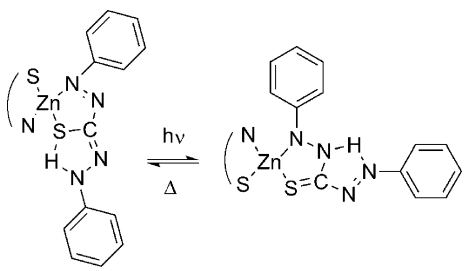

Figure 6. Structural isomerization of the HDz^- ligand involved in the photochromic equilibrium of $Zn(HDz)_2$ complex.

extent with X-ray data. On passing from the stable to the activated form, metal–ligand bond lengths undergo a slight increase. The obtained values are 2.330 vs 2.380 Å for the Zn–S distance, and 2.149 vs 2.161 Å for the Zn–N one. The ligand is almost planar in both cases, with the planes of the two phenyl rings forming a dihedral angle of 9.0 and 8.1° for the stable and the activated form, respectively. A total energy difference of 28.6 kcal mol^{-1} between the two forms was computed, a value appreciably higher than the photon energy necessary to activate the complex (488 nm, corresponding to 58.6 kcal mol^{-1}).

The spin-allowed excitation energies of both the stable form and the activated one proposed in Meriwether *et al*.[3] were computed by the TDDFT formalism. As regards the stable form, a strong absorption at 605 nm, corresponding to the $2^1B \leftarrow 1^1A$ excitation, was observed. The excitation energy is underestimated by 0.28 eV, a typical deviation for similar calculations.[49,50] The transition is polarized along the *y* axis, where the *z* axis is the symmetry axis of the molecule, and *x* is the axis passing through the sulfur atoms. Inclusion of solvent effects seems to play a less important role in comparison to the free ligand. This finding is not unexpected, since the specific ligand–solvent interactions are replaced by the ligand–metal ones, which are explicitly considered in the calculations. In the case of chloroform, the solvent used in NMR experiments, a rather weak red-shift to 571 nm was observed. Considering the activated form, the most intense low-energy transition ($\lambda = 747$ nm) still corresponds to an excitation to the 2^1B state. Thus, the first absorption peak is predicted to undergo a 142 nm red-shift upon activation, which is in fair agreement with the experimental value (78 nm). Diagrams showing the character of the transition in terms of monoelectronic excitations are displayed in Figs 7 and 8 for the stable and the activated isomer, respectively. Monoelectronic levels are grouped in pairs of almost unsplit *a*- and *b*-type symmetry combinations of the ligand orbitals. In both isomers, the LUMO and the LUMO + 1 corresponding to the final states have a main N–N π^* character, whereas the HOMO and the HOMO + 1 have a partial S–lone pair character. As a consequence, the considered transition can be classified as an $n \rightarrow \pi^*$ type. The narrower energy gap found for the activated form is in agreement with the higher wavelength of the absorption peak. Furthermore, an almost pure S–lone pair character characterizes the HOMO − 2/HOMO − 3 MOs of the stable form and the HOMO − 4/HOMO − 5 ones of the activated one. Nevertheless, a substantial contribution (14 and 8%) from monoelectronic transitions involving these MOs is predicated only for the stable isomer and not for the activated one, indicating a stronger charge-transfer character in the former case.

CONCLUSIONS

The present work was focused on a theoretical and experimental investigation on zinc(II) dithizonate, a complex

DOI: 10.1002/aoc

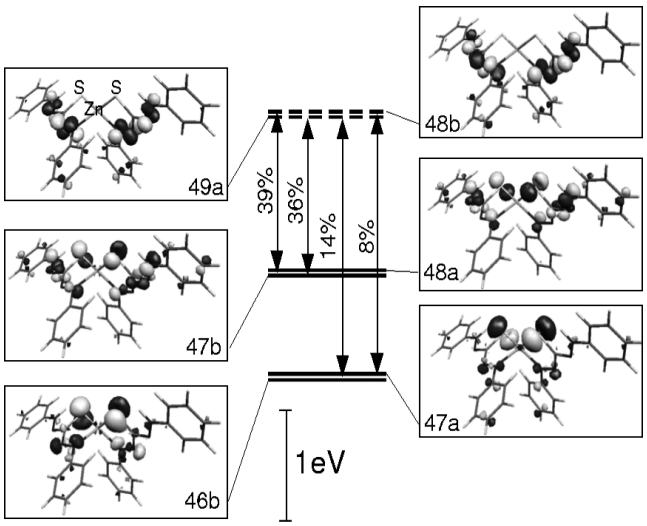

Figure 7. Main monolectronic contributions to the $2^1B \leftarrow 1^1A$ transition for the stable complex form. Solid/dashed lines refer to filled/empty levels. Energy separations of *a*–*b* symmetry combinations are slightly enhanced for sake of clarity.

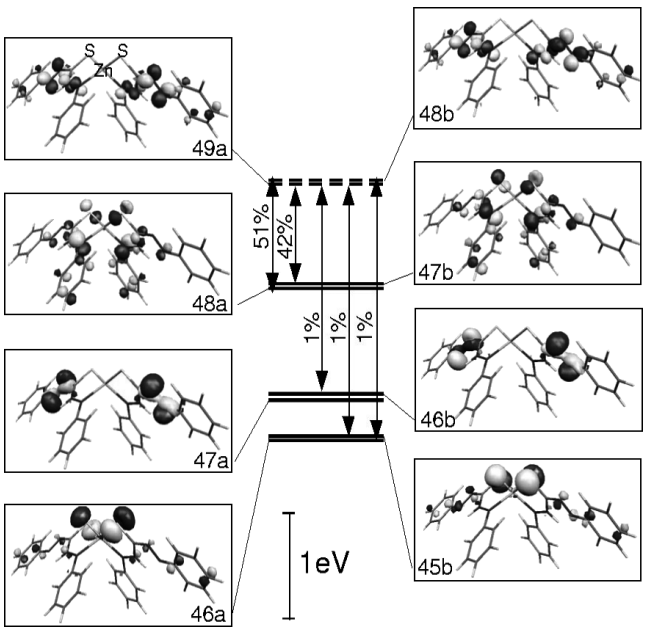

Figure 8. Main monoelectronic contributions to the $2^1B \leftarrow 1^1A$ transition for the activated complex form.

endowed with interesting optical properties. In particular, after a detailed structural characterization, the $Zn(HDz)_2$ behavior in solution, along with that of the free H_2Dz ligand, was studied by means of optical absorption and NMR spectroscopies and compared with the results obtained by DFT computation. Beside investigating the intramolecular enantiomerization process occurring in solution, this multi-technique approach has enabled light to be shed on the electronic structure and bonding of the stable complex form and data to be compared with those pertaining to the activated one involved in the photochromic equilibrium. Taken together, these results disclose interesting perspectives for the inclusion of $Zn(HDz)_2$ as *guest* in transparent oxide matrices, aimed at the development of advanced optical devices.

Acknowledgments

The National Research Council (CNR), University of Padova and INSTM are acknowledged for financial support. We are also indebted to research programs FISR-MIUR 'Molecular nanotechnologies for information storage and transmission', FIRB-MIUR—RBNE019H9K 'Molecular manipulation for nanometric machines', FIRB-MIUR—RBNE01YLKN 'Nano-organization of inorganic/organic hybrid molecules with magnetic and optical properties', PRIN-MIUR 2005 'Molecular architectures organized on inorganic and hybrid matrices', and FIRB-MIUR–RBNE033KMA 'Molecular compounds and hybrid nanostructured materials with resonant and non resonant optical properties for photonic devices'. Thanks are due to Dr Flavio Carli for useful help in the experimental work.

REFERENCES

1. Fabretti AC, Peyronel G. *J. Inorg. Nucl. Chem.* 1975; **37**: 603.
2. Math KS, Fernando Q, Freiser H. *Anal. Chem.* 1972; **36**: 1762.
3. Meriwether LS, Breitner EC, Sloan CL. *J. Am. Chem. Soc.* 1965; **87**: 4441.
4. Meriwether LS, Breitner EC, Colthup NB. *J. Am. Chem. Soc.* 1965; **87**: 4448.
5. Geosling C, Adamson AW. Gutierrez AR. *Inorg. Chim. Acta* 1978; **29**: 279.
6. Spevacek V, Spevackova V. *J. Inorg. nucl. Chem.* 1976; **38**: 1299.
7. McArdel CB. *Applied Photochromic Polymer Systems*, McArdle CB (ed.). Blackie: Glasgow, 1992.
8. Delaire JA, Nakatani K. *Chem. Rev.* 2000; **100**: 1817.
9. Atassi Y, Chauvin J, Delaire JA, Delouis JF, Fanton-Maltey I, Nakatani K. *Mol. Cryst. Liq. Cryst. Sci. Technol., Sect. A* 1998; **315**: 313.
10. Atassi Y, Chauvin J, Delaire JA, Delouis JF, Fanton-Maltey I, Nakatani K. *Pure Appl. Chem.* 1998; **70**: 2157.
11. Paci B, Nunzi JM, Sertova N, Petkov I. *J. Photochem. Photobiol., A* 2000; **137**: 141.
12. Sertova N, Petkov I, Nunzi JM. *J. Photochem. Photobiol., A* 2000; **134**: 163.
13. Nayak B, Gupta SN. *J. Polym. Sci.* 1995; **33**: 891.
14. Dahlberg SC, Reinganum CB. *J. Chem. Phys.* 1982; **76**: 5515.
15. Yamamoto Y, Yoshinaga T, Yamada S. *Bull. Chem. Soc. Jpn* 1936; **36**: 827.
16. Bax A, Subramian S. *J. Magn. Reson.* 1986; **67**: 565.
17. Otting G, Wütrich K. *J. Magn. Reson.* 1988; **76**: 569.
18. Drobny G, Pines A, Sinton S, Weitekamp D, Wemmer D. *Faraday Symp. Chem. Soc. B* 1979; **33**: 49.
19. Bax A, Summers MF. *J. Amer. Chem. Soc.* 1986; **108**: 2093.
20. Bodenhausen G, Kogler H, Ernst RR. *J. Magn. Res.* 1984; **58**: 370.
21. te Velde G, Bickelhaupt FM, van Gisbergen SJA, Fonseca Guerra C, Baerends EJ, Snijders JG, Ziegler T. *J. Comput. Chem.* 2001; **22**: 931.
22. Fonseca Guerra C, Snijders JG, te Velde G, Baerends EJ. *Theor. Chem. Acc.* 1998; **99**: 391.

DOI: 10.1002/aoc

23. ADF2002.01. SCM, Theoretical Chemistry, Vrije Universiteit, Amsterdam; http://www.scm.com.
24. Casida ME. *Recent Advances in Density Functional Methods*, Chong DP (ed.). World Scientific: Singapore, 1995.
25. van Gisbergen SJA, Snijders JG, Baerends EJ. *Comput. Phys. Commun.* 1999; **118**: 119.
26. Klamt A, Schuurman G. *J. Chem. Soc. Perkin Trans.* 1993; **2**: 799.
27. Pye CC, Ziegler T. *Theor. Chem. Acc.* 1999; **101**: 396.
28. Fischer E. *Liebigs Ann. Chem.* 1878; **190**: 67.
29. Laing M. *J. Chem. Soc. Perkin Trans.* 1977; **2**: 1248.
30. Pemberton JE, Buck RP. *J. Raman Spectr.* 1982; **12**: 76.
31. Hutton AT, Irving HMNH. *J. Chem. Soc. Chem. Commun.* 1981; 735.
32. Richter W, Gdanitz H, Röbish G. *Z. Chem.* 1985; **25**: 270.
33. Langbein H, Nöske R, Röbish G. *Z. Chem.* 1983; **23**: 149.
34. Grummt UW, Nöske R, Röbish G. *Z. Chem.* 1983; **23**: 300.
35. Grummt UW, Langbein H, Nöske R, Röbish G. *Z. Chem.* 1983; **23**: 56.
36. Wagler H, Koch H, Flachowsky J. *Z. Chem.* 1984; **21**: 98.
37. Schönherr T, Linder R, Rosellen U, Schmid V. *Int. J. Quantum Chem.* 2002; **86**: 90.
38. Gutowsky HS, Holm CH. *J. Chem. Phys* 1956; **25**: 1228.
39. Takeda M, Stejiskal EO. *J. Amer. Chem. Soc.* 1960; **82**: 25.
40. Rogers MTM, Woodbrey JC. *J. Chem. Phys.* 1962; **66**: 540.
41. Allerhand A, Gutowsky HS, Jonas J, Meinzer RA. *J. Am. Chem. Soc.* 1966; **88**: 3185.
42. Perrin CL. *Magn. Reson.* 1988; **26**: 224.
43. Perrin CL, Dwyer TJ. *Chem. Rev.* 1990; **90**: 935.
44. Abel EW, Coston TPJ, Orrell KG, Sik V, Stephenson D. *J. Magn. Res.* 1986; **70**: 34.
45. Macura S, Ernst RR. *Mol. Phys.* 1980; **41**: 95.
46. Perrin CL, Gipe RK. *J. Am. Chem. Soc.* 1984; **106**: 4036.
47. Eaton SS, Holm RH. *Inorg. Chem.* 1971; **10**: 1446.
48. Nivorozhkin AL, Sukholenko EV, Nivorozhkin LE, Borisenko NI, Minkin VI, Grishin YK, Diachenko OA, Takhirov TG, Tagiev DB. *Polyhedron* 1989; **8**: 569.
49. Bauernschmitt R, Ahlrichs S. *Chem. Phys. Lett.* 1996; **56**: 454.
50. Casida ME, Jamorski C, Casida KC, Salahub DR. *J. Chem. Phys.* 1998; **108**: 4439.

DOI: 10.1002/aoc